# Long-Period Ground Motion in the Arabian Gulf from Earthquakes in the Zagros Mountains Thrust Belt

ARBEN PITARKA,[1] ABDULLAH AL-AMRI,[2] MICHAEL E. PASYANOS,[1] ARTHUR J. RODGERS,[1] and ROBERT J. MELLORS[1]

*Abstract*—The Arabian Gulf is adjacent to the Zagros Mountains, one of the most seismically active regions in the world. We observe that broadband seismic records of Zagros earthquakes recorded on the Arabian side of the Gulf display long-duration surface waves. While shorter periods (<1 s) are attenuated from crossing the deep sediments (>10 km) of the Gulf basin, the long-period energy is enhanced and transmitted efficiently. Consequently, large earthquakes in the Zagros could result in amplified ground motions at long periods (2–10 s) relative to average behavior. Such ground motions are of concern for large engineered structures, such as tall buildings and long bridges with resonant periods in the same period range. Here we present results of investigations of the characteristics of ground motions recorded on the western shore of the Gulf from selected earthquakes in the Zagros Mountains region. Exceptionally, long-duration seismic waves, as compared with standard models, are shown to occur with periods of 2–10 s. This may be due to waveguide effects in the deep sedimentary basin structure of the Arabian Platform. In addition to analyzing recorded ground motion we performed 3D wave propagation simulations using a finite difference method and experimental velocity models of the Gulf, with different shallow sedimentary layers structures. The simulation results confirm our hypothesis that long-period waves with extremely long duration and relatively large amplitudes are caused by the geometry of the basin sedimentary layers and, to some extent, by shallow earthquake depths. Combined effects of basin edge geometry with sharp velocity contrasts and shallow sources (<10 km) on the eastern side of the Arabian Gulf can cause large long-period ground motion on the western side of the Gulf. In contrast, the short-period content of ground motion (<2 s) at long distances is relatively weak. This is mainly due to wave propagation scattering and attenuation in the shallow sedimentary layers of the Gulf basin.

[1] Atmospheric, Earth and Energy Division, Lawrence Livermore National Laboratory, 7000 East Avenue, L-046, P.O. Box 808, Livermore, CA 94551, USA. E-mail: pitarka1@llnl.gov

[2] Department of Geology and Geophysics, King Saud University, Riyadh 11451, Saudi Arabia.

## 1. Introduction

The Persian/Arabian Gulf (hereafter referred to as the Arabian Gulf, or simply Gulf) lies near the boundary of the Arabian and Eurasian Plates. While the Gulf is mostly aseismic, the Arabian Peninsula is surrounded by regional seismic sources in the tectonically active areas of Iran and Turkey to the northeast, the Red Sea Rift bordering the Shield to the southwest, and the Dead Sea Transform fault zone to the north (JOHNSON 1998; AL-AMRI 2013). These seismic sources control the majority of the seismic hazard in and around the Arabian Peninsula. Throughout recorded history, many damaging earthquakes have occurred along the Arabian Plate boundaries. These events have damaged buildings, and resulted in injuries and fatalities (AMBRASEYS 1988; AMBRASEYS et al. 1994; ALSINAWI 1986).

The Zagros Mountains, which are located on the northeast side of the Arabian Gulf, is a very seismically active region. Large earthquakes in this region are capable of producing significant ground motion on the southwest side of the Gulf. Recent examples are the 2005 M5.7 and the 2008 M6.1 Qeshm Island earthquakes, which were particularly strongly felt in highrise buildings in the urban centers along the Gulf. The Makran subduction zone, located at the southern end of the plate boundary, where the Arabian plate subducts underneath the Eurasian plate, is capable of magnitude 7 and 8 events. These will also produce strong shaking along the Gulf. A repeat of the November 1945 M8.1 Makran earthquake will cause long-duration and high-amplitude ground motion along the Gulf.

In this paper, we analyze ground motions recorded on the Arabian side of the Gulf using a mix of observations and full waveform 3D modeling. In

particular, we examine the amplitude of long-period surface waves, which may present a hazard to large structures with resonant periods of 2–10 s. A number of large structures, such as high-rise buildings and bridges, exist in populated areas along the Gulf, and more are planned to be build. As the population increases and new areas are developed, the seismic risk to human life and infrastructure increases. In order to fully capture the seismic hazard of the Arabian Peninsula, we must understand the effects of the regional 3D underground structure on wave propagation. These effects cannot not be fully predicted by simply adopting GMPEs that are developed for other regions.

In this article we briefly describe the tectonic setting and crustal structure of the region. Then we discuss characteristics of ground motion from recent events. Finally, we investigate structural effects on ground motion by modeling 3D anelastic wave propagation using a finite difference method.

## 2. Tectonics and Seismicity of the Arabian Platform Region

Figure 1 shows the location of the study area which includes the Arabian Gulf. The Arabian Plate is under-thrusting the southern Eurasian margin along the Zagros Mountains Thrust on the northwest side of the Arabian Gulf. Further southeast the oceanic crust continues to subduct under the southern region of the Eurasian plate. The transition zone between the continental underthrusting and oceanic subduction consists of complex strike-slip faulting associated with some thrust faulting.

The Arabian Peninsula consists of exposed Paleozoic shield in the west, but is covered by sediments in the east (Arabian Platform). These sediments dip E–NE gently into the thick basin sediments of the Arabian Gulf. In general, the crust is 40–45 km thick and may be slightly thicker in the east. The velocity of the upper mantle is about
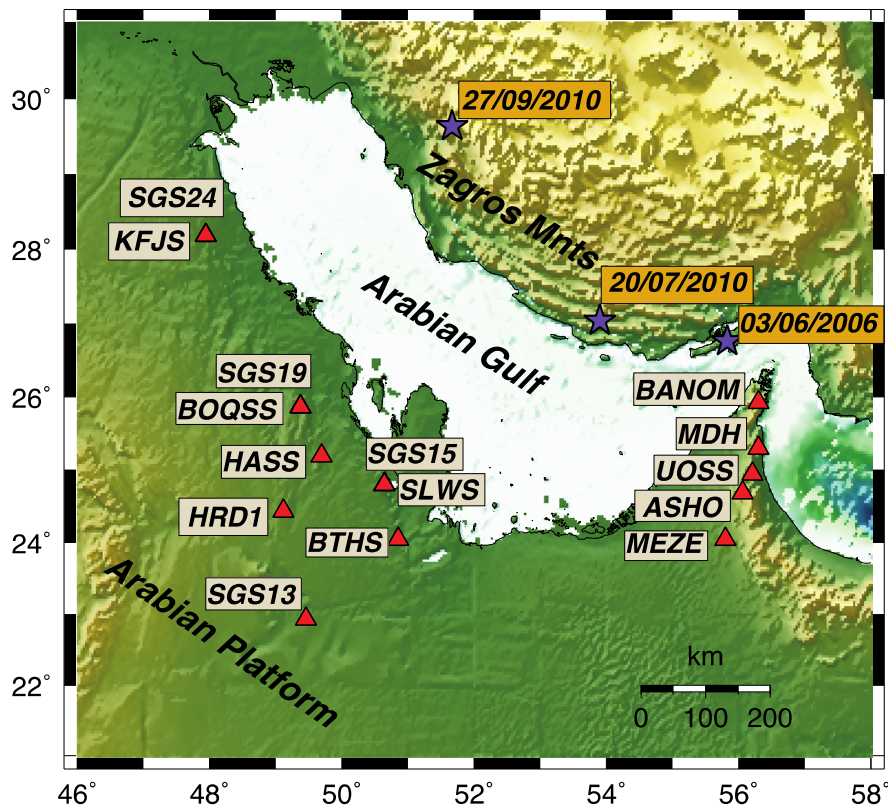


Figure 1
Map of the study region. *Triangles* show the location of seismic stations, and *stars* show the location of three earthquakes used in analysis of recorded ground motion

8.2 km/s (AL-AMRI 1998; AL-AMRI et al. 1999; ROD-GERS et al. 1999; TKALČIĆ et al. 2006). GÖK (2008) showed that sedimentary basin structure varies across the Arabian Platform, but crystalline crust is largely uniform in thickness and wavespeed.

Regional seismic phases display considerable azimuthal variation. High-frequency regional S-wave phases are quite different for paths crossing the Arabian Shield than those crossing the Arabian Platform (MELLORS et al. 1999; AL-DAMEGH et al. 2004). In particular, the mantle Sn phase is nearly absent for paths crossing parts of the Arabian Shield, while the crustal Lg phase has abnormally large amplitude. The situation is reversed for paths crossing the Platform and Gulf, where Lg tends to show lower amplitudes, but Sn propagates effi-ciently. These variations appear to be due to a combination of variations in mantle attenuation and crustal structure (RODGERS et al. 1997). AL-DAMEGH et al. (2004). observed low $Q_{Pn}$ (<100 at 1.5 Hz) along the western coast of the Arabian Plate and along the Dead Sea fault system. Higher $Q_{Pn}$ values of the order of 400 were observed within the Ara-bian Shield and Platform at the same frequency. Similar patterns of crust and upper mantle $Q_p$ and $Q_s$ in the Arabian Shield and Arabian Platform are found by PASYANOS et al. (2009) in their model of P-wave and S-wave attenuation in the Middle East region using multiphase (Pn, Pg, Sn, Lg) attenuation tomography.

Because of the limited amount of recorded ground motion data and poor seismic station cov-erage, the seismicity of the Gulf region is not well characterized. The seismicity is very low in the Arabian Gulf. In contrast, the seismicity is very high in the Zagros Mountains thrust belt that extends for a distance of about 1,500 km in a northwest–southeast direction. The earthquakes in the Zagros define a zone of about 200 km wide that runs par-allel to the fold belt. The majority of earthquakes occur in the crustal part of the Arabian plate that is underthrust along the folded belt. Magnitude 5 earthquakes are frequent and magnitude 6 may occur every year. The nature of deformation across this zone is complex, involving both thrust and strike-slip as indicated by earthquake focal mecha-nisms (TALEBIAN and JACKSON 2004).

## 3. Analysis of Recorded Long-Period Ground Motion in the Gulf Region

The Arabian Gulf lies on a deep sedimentary basin. The sedimentary layers dip eastward, reaching a depth of up to 8 km adjacent to the Zagros. Figure 2 shows a map of depth to basement in the region proposed by LASKE and MASTERS (1997). The deep structure of the Gulf is composed of geologically old and consolidated sediments with moderately high shear velocities (e.g., PASYANOS et al. 2014). How-ever, younger sediments near the surface have much lower velocities and probably high attenuation. ROD-GERS et al. (2006) and AL-AMRI et al. (2008) demonstrated that the sedimentary layers of the Arabian Gulf cause higher amplitude and longer duration ground shaking then normally observed in a continental crustal structure. The complex basin structure is of particular concern for the earthquake hazard in the Gulf.
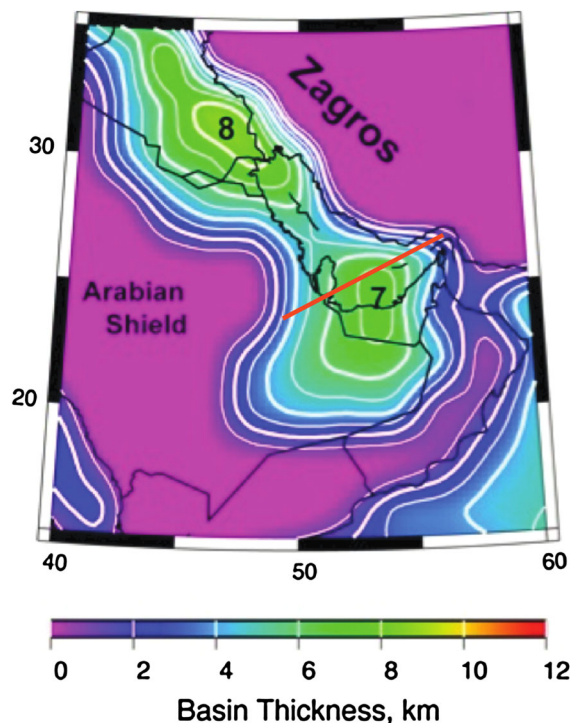


Figure 2

Sediment thickness of the Arabian Gulf and surrounding region (LASKE and MASTERS 1997). *Red line* indicates the location of the velocity model cross section shown in Fig. 7. *Bold numbers* indicate maximal basin depth in km

This study is an attempt to analyze quantitatively ground motion characteristics observed in the western side of the Arabian Gulf from earthquakes in the Zagros Mountains and Iranian Plateau. In particular, we focused on long-period (1–10 s) ground motion waveforms. Figure 3 shows typical time histories of ground motion velocity recorded at seismic stations in eastern Saudi Arabia from the M5.1 June 3, 2006 earthquake (see Fig. 1 for its location). The north–south component, corresponding most naturally with the transverse component of ground motion is shown for two frequency ranges: (a) 0.02–0.05 Hz (50–20 s) and 0.1–1.0 Hz (10–1 s). The very long period band (20–50 s) shows the surface waves arriving between 3.5 and 3.0 km/s, as expected for normal continental paths at regional distance. The surface wave is relatively simple with a short duration, and is normally dispersed, as expected. However, at shorter periods of 1–10 s the ground motion shows an unexpectedly long duration of up to hundreds of seconds and at lower group velocities. This long duration shaking will cause increased cyclical loading on large engineered structures, such as high-rise buildings, bridges, and pipelines, that are sensitive to seismic motion in the period range of 1–10 s. Similar observations have been made for other earthquakes recorded at station HASS for which the wave path crosses the thick sedimentary cover in the Persian/Arabian Gulf. The observed, extraordinarily long duration is likely due to a waveguide effect from the deep sedimentary structure of the basin which enhances long-period ground motion (e.g., MELLORS et al. 1999). Seismic waveforms are affected by both wave path and source effects (e.g., PITARKA et al. 1998). Path effects are a consequence of heterogeneous underground structure and surface topography. Lateral and vertical variations in velocity cause dispersion, diffraction, and reflections, all of which affect wave amplitude and duration. The effect of wave scattering due to small-scale heterogeneities (e.g., FRANKEL and CLAYTON 1986) is significant at intermediate and high frequencies (0.05–1 Hz). In general, wave attenuation is stronger in sedimentary basins than in basement and crystalline crust. However, the increased duration and relatively large amplitude of ground motion recorded along the west coast of the Gulf region suggests that seismic attenuation in the Gulf basin is very low for these periods.



**(a)** Band-pass 0.02-0.05 Hz
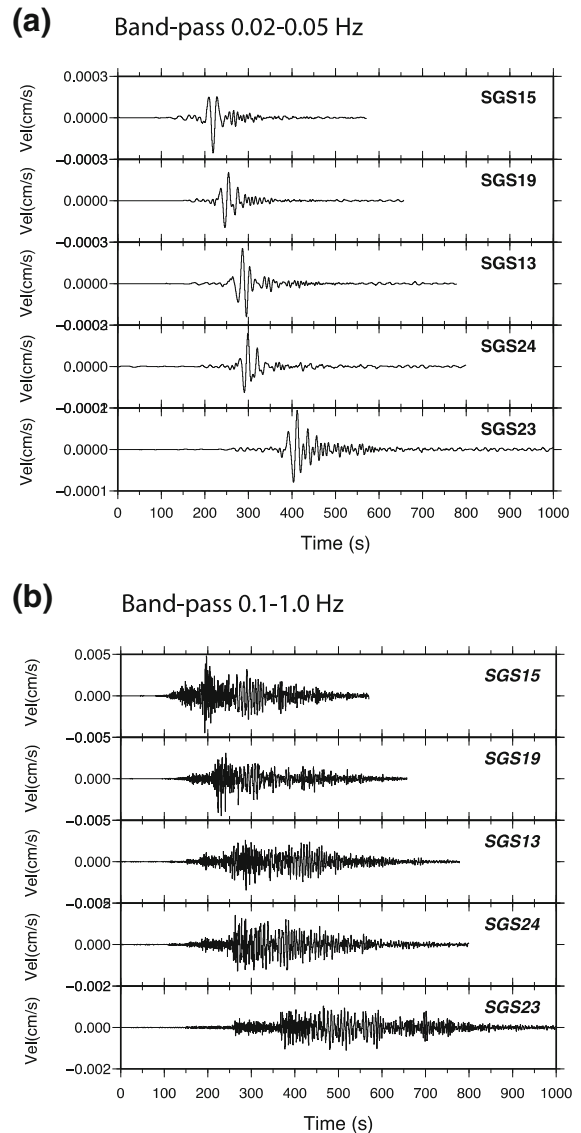
**(b)** Band-pass 0.1-1.0 Hz

Figure 3
Seismograms for June 3, 2006 earthquake recorded at stations in eastern Saudi Arabia filtered **a** 0.02–0.05 Hz (50–20 s), and **b** 0.1–1.0 Hz (10–1 s). Note that the 1–10 s period band shows an unusual long duration signal of more than 300 s

## 4. Acceleration Response Spectra

We used ground motions from several earthquakes in the Zagros thrust belt recorded at stations on the west coast of the Gulf to investigate the effects of the Gulf basin structure on long period wave propagation. The location of the seismic stations is shown in Fig. 1. Although the number of stations is

limited, their location allows for a comparison of wave propagation effects along different E–W directions across the basin.

In the absence of calibrated GMPEs for the Gulf region we analyzed the spectral characteristics of ground motion in the region by comparing recorded spectral acceleration with the GMPEs developed by CAMPBELL and BOZORGNIA (2008) and BOORE and ATKINSON (2006), hereafter referred to as CB08 and BA06, respectively. These equations are based on ground motion data from earthquakes around the world. CB08, a Next-Generation Attenuation equation, was developed for earthquakes in active, shallow crustal structures. It is controlled by various parameters, including magnitude, distance, type of rupture, and basin depth (depth to layer with $V_s = 2.5$ km/s). Because of the limited amount of good quality data at long distances the standard deviation of this equation is large at distances longer than 200 km and periods shorter than 3 s. On the other hand, BA06 is constrained better at large distances. BA06 was developed for eastern North America, which in some respects resembles the sediments/shield and tectonically stable structure of eastern Arabian Platform.

We compared the spectral ratio between the recorded and predicted spectral acceleration for 5 % damping at different periods. Figure 4 shows the comparison with CB08 as a function of distance. Not all the earthquakes considered in this comparison were well recorded at all stations. We only show results for stations that produced good quality data from at least two earthquakes. The predicted spectral acceleration was computed for a depth to basement of 3.5 km. The spectral ratios clearly show different behaviors at different periods. The recorded spectral acceleration is much higher than the one predicted by the GMPEs in the 10 s period. It is comparable in the 5 s period and much lower in the 1 s period. The comparison with BA06 has a similar trend (Figs. 5, 6). In relative terms these results suggest that, in general, waves crossing the Gulf basin from the east are attenuated much less than expected at long periods. They are attenuated more than expected at shorter periods. Some of the amplification could be due to the basin structural effects, which for a deep basin such as the Gulf basin, are expected to be stronger at long periods. Long-period surface waves, which dominate the 10-s spectral response, are affected by the entire basin structure since they penetrate through the upper 10 km of the crust. On the other hand, shorter period waves (periods shorter than 1 s) have energy concentrated in the shallow basin sedimentary layers, and their shorter wavelengths are more susceptible to wave scattering effects compared to longer period waves. Consequently, short-period waves generated by earthquakes on the east coast of the Gulf are more prone to attenuation. Their amplitude is relatively small when they reach the west coast of the Gulf. The departure of the recorded spectral amplitudes from the GMPEs does not seem to correlate with source distance.

We also observed a significant dissimilarity among acceleration response spectra from three selected earthquakes recorded at different stations. This is illustrated using ground motion time histories from the M5.3 2006/06/03, M5.7 2010/07/20, and M5.9 2010/09/27 earthquakes, corrected for geometrical spreading and radiation pattern. The earthquake locations are indicated in Fig. 1, and the comparison is shown in Fig. 8. In the case of the 2006/06/03 earthquake, the response spectra are similar for periods longer than 3 s, except for station SGS24, which recorded much lower ground motion. The similarity breaks down at shorter periods. The largest difference is obtained in the period range of 0.5–3 s between stations SGS15 and SGS13 which have a similar direction from the event, but very different source distances. Besides having a longer distance, SGS13 is located outside the basin. Our interpretation of the observed similarities between the stations for periods longer than 3 s and dissimilarities for periods shorter than 3 s is that, while the energy carried by longer period waves leaks outside the basin as they propagate toward the west, short-period energy is trapped in the basin sedimentary layers. Consequently, long-period waves on the west coast of the Gulf will maintain their large amplitude and duration regardless of the station's location relative to the basin. In contrast, the amplitude of short-period waves will mostly depend on whether the site is within or outside the basin.

The most significant feature of the response spectra from the 2010/07/20 earthquake is the
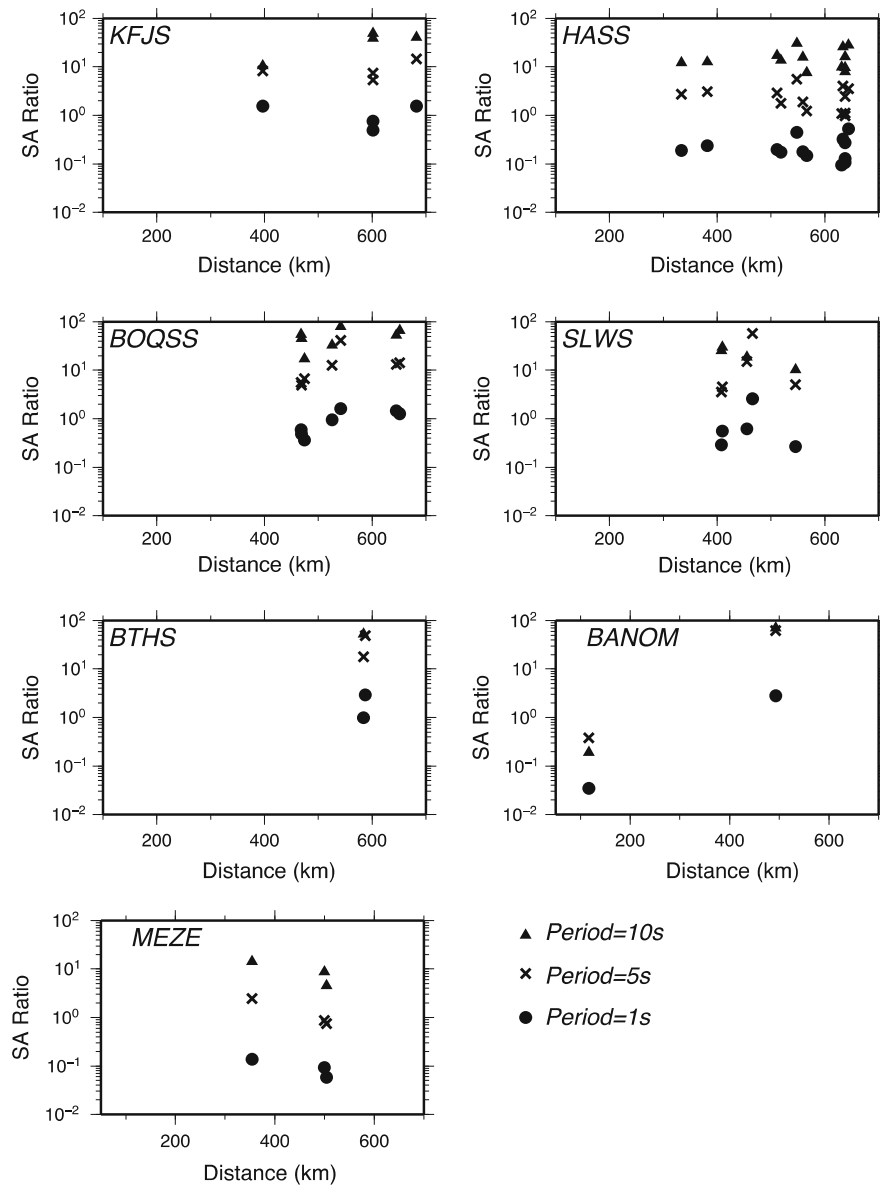
Figure 4
Spectral acceleration ratios of recorded and predicted ground motion for the geometric mean horizontal component at periods 1 s (*solid circle*), 5 s (*x*'s), and 10 s (*triangles*), and 5 % damping. The predicted ground motion was computed using the GMPE of (CAMPELL and BOZORGNIA 2008). The station names are shown in each panel

difference in spectral amplitudes between stations SLWS, KFJS, and BOQS. The three stations are on wave paths that cross the deepest parts of the basin. However, at SLWS the spectral acceleration is much larger in the period range 2–20 s. In contrast, the spectral amplitudes at BOQSS are very similar to spectral amplitudes at KFJS, which has a much longer epicentral distance, and is located on different wave path. The spectral differences between SLWS and BOQSS are an indication of path-specific wave propagation effects on ground motion along different paths across the basin. The basin depth, and probably its geometry, along the two wave paths changes considerably.

A similar trend in ground motion variability is seen for the 2010/09/27 earthquake. Although the
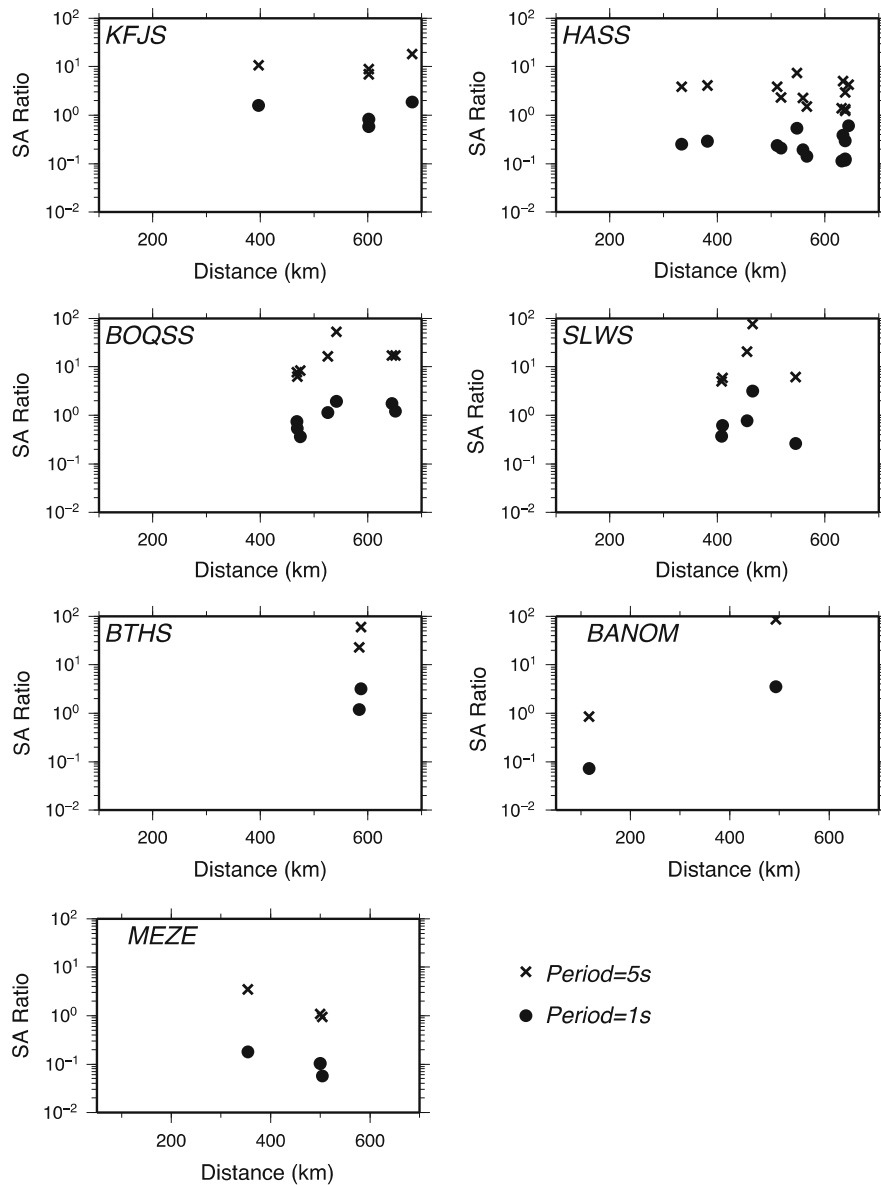
Figure 5
Spectral acceleration ratios of recorded and predicted ground motion for the geometric mean horizontal component at periods of 1 s (*solid circles*), 5 s (*x*'s), and 5 % damping. The predicted ground motion was computed using the GMPE of Boore and Atkinson (2006), developed for eastern North America. The station names are indicated in each panel

epicentral distances of stations BOQSS, SLWS, and HRD1 are twice as large as that of UOSS, the observed spectrum at these stations is at least a factor of 10 larger, especially in the period range of 0.1–3 s. At periods longer than 5 s the spectral amplitudes at UOSS exceed those at other stations. UOSS is located in the shallow part of the basin has a relatively flat spectrum on a broad period range. The similarities and dissimilarities among stations suggest that path-specific effects can selectively amplify certain periods at sites in the western Gulf coast.

Based on these observations, we conclude that the deep sedimentary structure in the Gulf acts as a waveguide that enhances long-period seismic wave amplification. In contrast, the shallow sedimentary layers attenuate high frequency waves, either due to
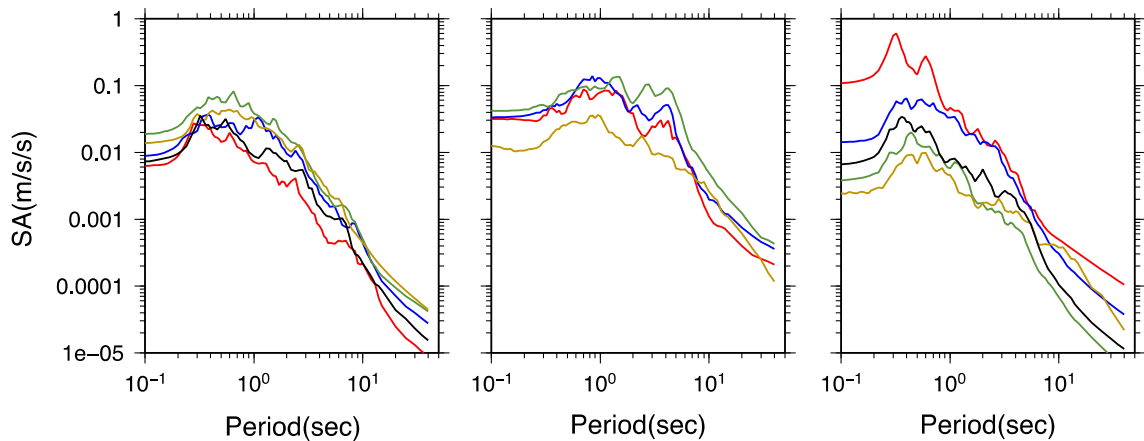
Figure 6
Geometrical mean of horizontal ground motion acceleration response spectra from M5.3 2006/06/03 earthquake (*left panel*), M5.7 2010/07/20 earthquake (*middle panel*), and M5.9 2010/09/27 earthquake (*right panel*), recorded at selected stations in the Gulf region. The spectra are corrected for the radiation pattern and geometrical spreading. The names of the stations are shown in each panel

wave scattering or due to low quality factor in the shallow sedimentary layers. Therefore, the knowledge of the basin structure on a broad scale range and validated modeling of its effects on wave propagation is crucial in predicting ground motion in the west coast of the Gulf.

## 5. Simulation of Basin Effects on Long-Period Ground Motion

The current knowledge of crustal structure in the Gulf region is limited to large-scale features that are expected to affect the amplitude and duration of long-period ground motion. New crustal models of the region are under development. PASYANOS *et al.* (2014) have recently developed a crustal model that has a higher resolution compared to existing models such as CRUST5.1 (MOONEY *et al.* 1998) and CRUST2.0 (BASSIN *et al.* 2000). In order to test our hypothesis of a basin wave guide to explain observed features of ground motion we investigated 3D wave propagation in the Gulf region using different basin models. We developed three experimental basin models representing different basin edge geometries and spatial extensions of surface sedimentary layers in the eastern and western parts of the Gulf. These features are not resolved in the current crustal models. The thickness of the basin was constrained by the basin

structure reported by (LASKE and MASTERS 1997). Figure 7 shows E–W vertical cross sections of the velocity models. In Model 1 the surface sedimentary layer continues across the entire model. In Model 2 the lateral extent of the surface sedimentary layer is limited toward the west. In Model 3 the geometry of the eastern basin edge is modified so that it can better channel the seismic energy coming from the seismic source below. The seismic velocity is the same for each model. The model dimensions are 800 km × 300 km × 90 km, and the top sedimentary layer has the properties: $V_p = 2.2$ km/s, $V_s = 1.2$ km/s, density 2 g/cm$^3$, $Q_P = 200$ and $Q_s = 100$.

We used WPP, a computer program developed at Lawrence Livermore National Laboratory (PETERSSON and SJOGREEN 2010a), to model three-dimensional anelastic wave propagation. WPP uses a second-order anelastic finite difference method (NILSSON *et al.* 2007) with mesh refinement (PETERSSON and SJOGREEN 2010b) and a curvilinear grid for treating non-planar, free-surface boundary conditions (APPELO and PETERSSON 2008). The code is parallelized, and has been used to model ground motion from large earthquakes

Figure 7 ▶
Vertical cross-sections of four velocity models used in the simulation of basin generated waves. The *star* indicates the location of the double-couple point source, and *triangles* indicate the location of receivers used in computing velocity ground motion. The location of the cross-section is indicated in Fig. 2
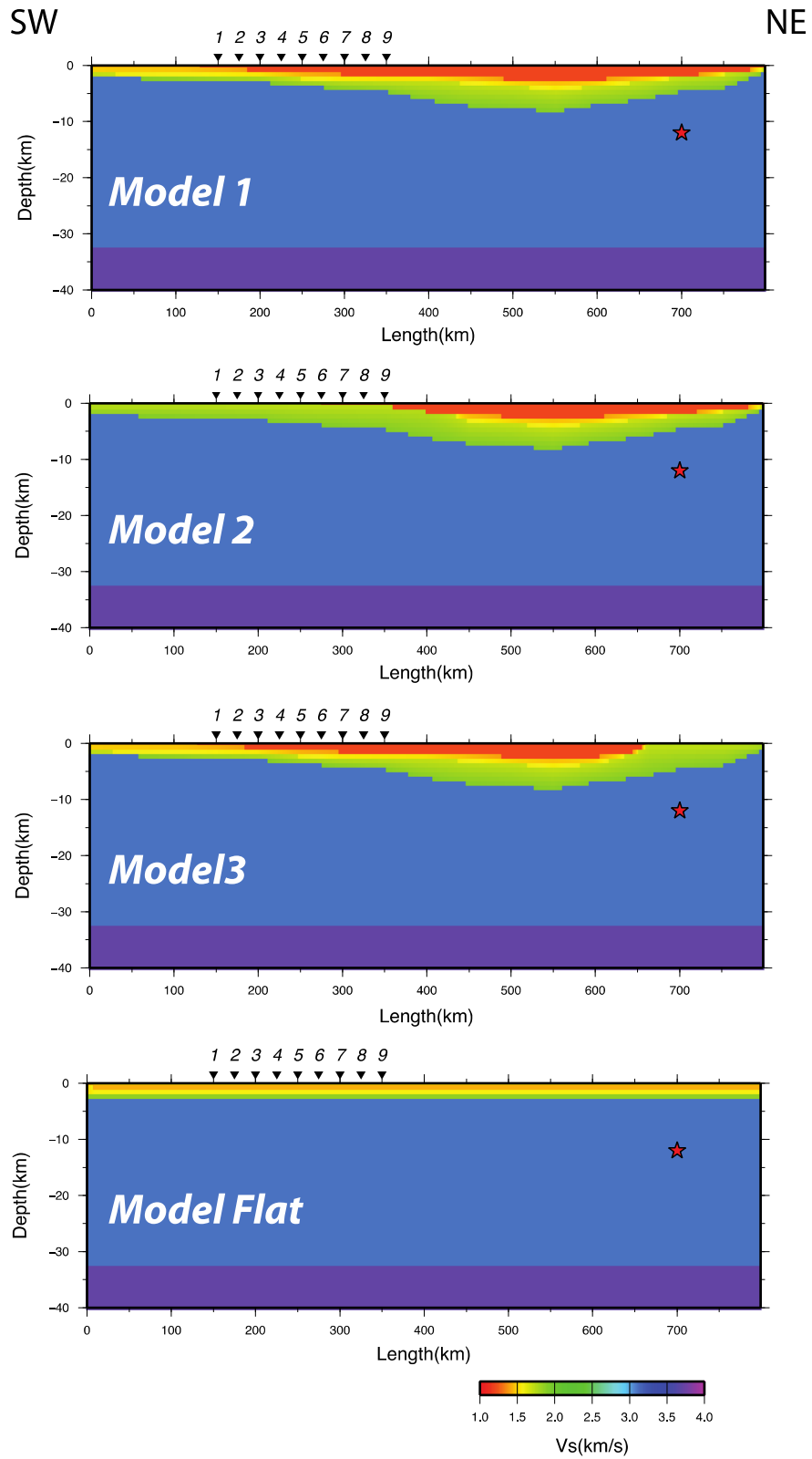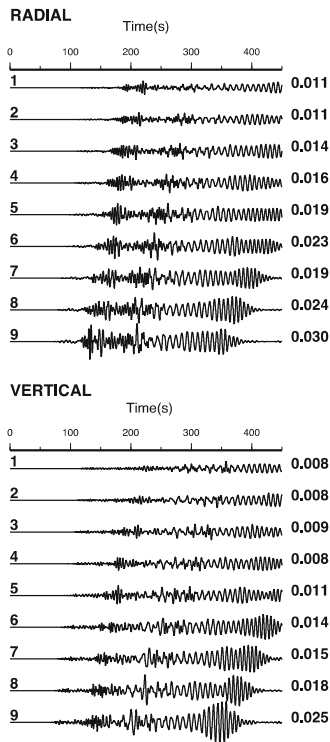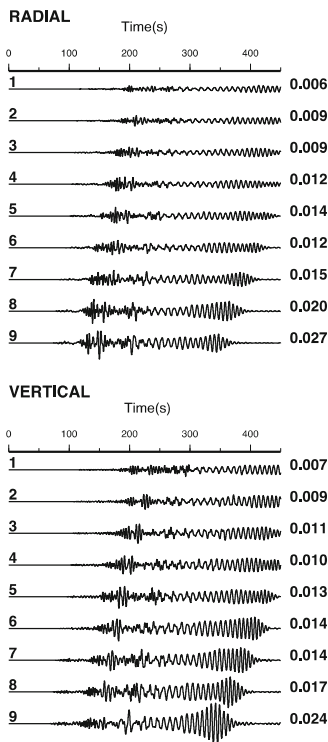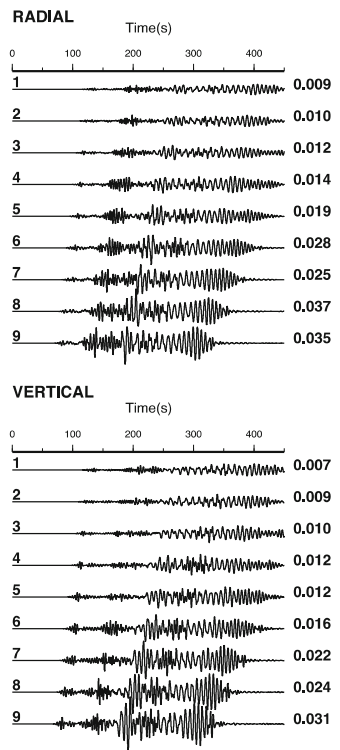
**(a)**

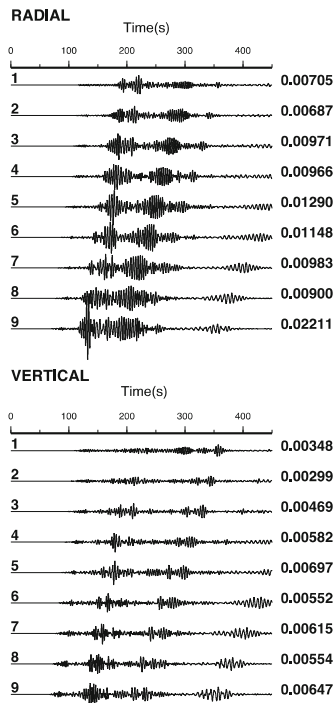**Model1**  Velocity (cm/s, 0.01 – 0.3 Hz)　　　**Model2**  Velocity (cm/s, 0.01 – 0.3 Hz)　　　**Model3**  Velocity (cm/s, 0.01 – 0.3 Hz)
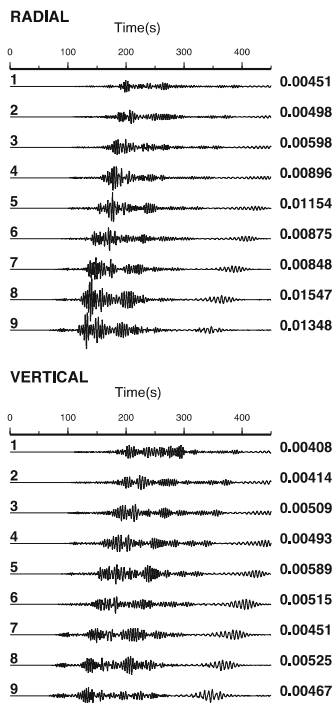


**(b)**

**Model1**  Velocity (cm/s, 0.2 – 0.3 Hz)　　　**Model2**  Velocity (cm/s, 0.2 – 0.3 Hz)　　　**Model3**  Velocity (cm/s, 0.2 – 0.3 Hz)
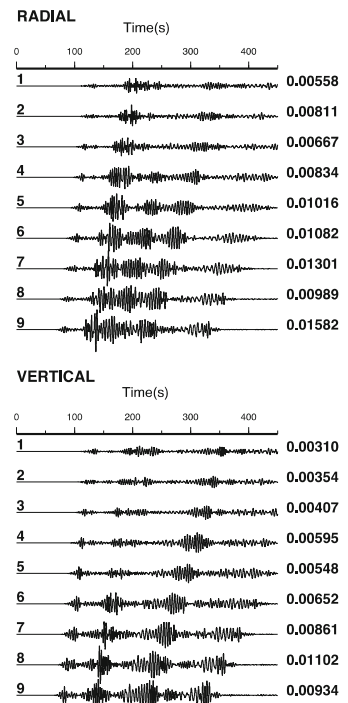
◄

Figure 8

**a** Synthetic velocity seismograms computed for a double-couple point source with a thrust mechanism using Model 1 (*left panels*), Model 2 (*central panels*), and Model 3 (*right panels*). The seismograms are band-pass filtered at 0.01–0.3 Hz. The number on the left of each seismogram indicates the peak amplitude in cm/s. **b** Synthetic velocity seismograms computed for a double-couple point source with a thrust mechanism using Model 1 (*left panels*), Model 2 (*central panels*), and Model 3 (*right panels*). The seismograms are band-pass filtered at 0.2–0.3 Hz. **c** Same as Fig. 8a, but band-pass filtered at 0.01–0.05 Hz

in California, such as the 1906 San Francisco earthquake (e.g., AAGAARD *et al*. 2008).

We used a grid spacing of 200 m in the top 10 km of the model, and 400 m in the region below. The numerical scheme used in the finite difference code is proven to be accurate for a minimum of 15 grid nodes per wavelength, which corresponds to a maximum frequency of 0.4 Hz. Nevertheless, in our analysis of simulated ground motion we used a maximum frequency of 0.3 Hz. We computed velocity seismograms at a linear array of stations,

indicated in Fig. 7, for an M5.4 earthquake using a double-couple point source with a thrust mechanism, which is typical for earthquakes in the Zagros region. The source has a depth of 12 km, and a Gaussian-type slip velocity function with a corner frequency of 1 Hz.

Figure 8a compares ground motion velocity seismograms computed with Model 1, Model 2, and Model 3, band-pass filtered at 0.01–0.3 Hz. Figure 8b and c show the same comparison, but in the frequency ranges of 0.1–0.3 Hz (2.5–10 s period range) and 0.02–0.05 Hz (20–50 s period range), respectively. We show the radial and vertical components of ground motion, which is dominated by basin-induced waves. Because of the predominant thrust mechanism of the source, the transverse component, not shown here, has much smaller amplitude. Note that the epicentral distances of receivers 1 and 2 are longer than 500 km. They fall within the source distance range of the seismic stations located on the west side
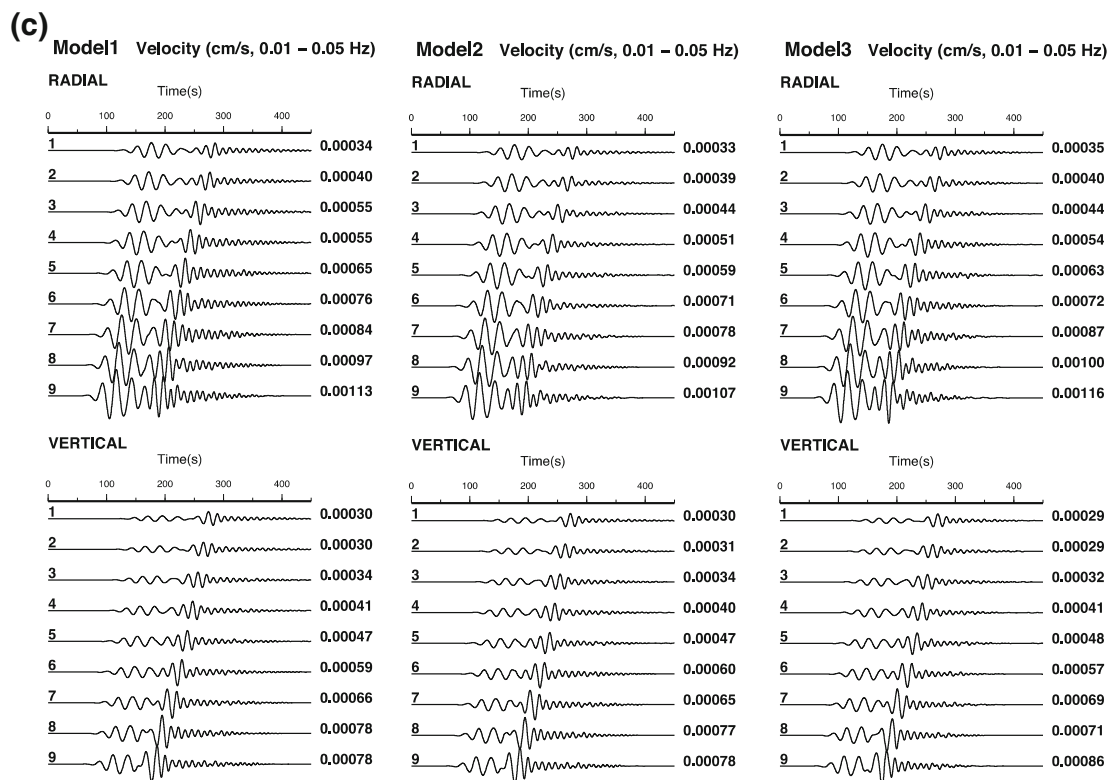


Figure 8
continued
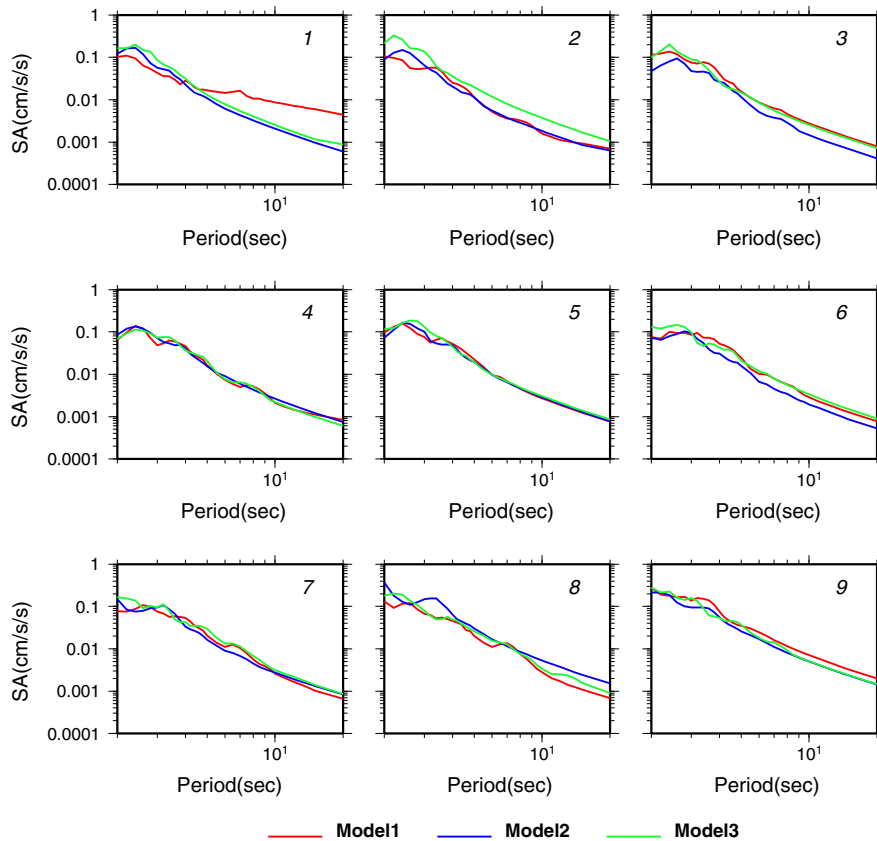
Figure 9
Comparison of acceleration response spectra of simulated ground motion for Model 1 (*red traces*), Model 2 (*blue traces*), and Model 3 (*green traces*)

of the Gulf. The other receivers were used to analyze the propagation of basin surface waves.

The ground motion in both radial and vertical components is dominated by dispersive basin surface waves that are trapped in the sedimentary layers. The basin-trapped waves are seen in different wave trains with group velocities that depend on basin layer velocity. The simulations reproduce the exceptionally long duration of ground motion of more than 350 s that is observed in the recorded data. Our simulation demonstrates that due to basin wave guiding, the amplitude of surface waves and their frequency content depends on the overall velocity structure of the basin. In general, Model 3 produces the largest ground motion, and Model 2 produces the weakest ground motion. This characteristic is more pronounced in the frequency range of 0.1–0.3 Hz (see

Fig. 8b). In contrast, in the period range of 20–50 s ground motion at very long periods is dominated by surface waves, and the three basin models produce very similar waveforms (Fig. 8c). This is not surprising since the three models have the same basin geometry and velocity background.

The most significant manifestation of basin-guided waves is seen in the comparison of simulated waves in the period range of 2.5–5 s (0.2–0.3 Hz). In this period range the waveforms vary among the models. The variation suggests that ground motion is sensitive to small-scale structural features. For example, compared to Model 1, Model 3, which has a sharper edge in the east side of the basin, produces larger ground motion, especially at stations 1 and 2. Stations 1 and 2 record waves that travel across the shallow part of the basin structure. The geometry of

**3D**                                                    **1D**

**Model1**  Velocity (cm/s, 0.01 − 0.3 Hz)          **Model Flat**  Velocity (cm/s, 0.01 − 0.3 Hz)

RADIAL                                                RADIAL

Time(s)                                               Time(s)

0      100    200    300    400                       0      100    200    300    400

1 ———————                           0.011             1 ———————                           0.021

2 ———————                           0.011             2 ———————                           0.023

3 ———————                           0.014             3 ———————                           0.024

4 ———————                           0.016             4 ———————                           0.025

5 ———————                           0.019             5 ———————                           0.027

6 ———————                           0.023             6 ———————                           0.030

7 ———————                           0.019             7 ———————                           0.033

8 ———————                           0.024             8 ———————                           0.036

9 ———————                           0.030             9 ———————                           0.039

VERTICAL                                              VERTICAL

Time(s)                                               Time(s)

0      100    200    300    400                       0      100    200    300    400

1 ———————                           0.008             1 ———————                           0.018

2 ———————                           0.008             2 ———————                           0.020

3 ———————                           0.009             3 ———————                           0.021

4 ———————                           0.008             4 ———————                           0.022

5 ———————                           0.011             5 ———————                           0.024

6 ———————                           0.014             6 ———————                           0.025

7 ———————                           0.015             7 ———————                           0.028

8 ———————                           0.018             8 ———————                           0.030

9 ———————                           0.025             9 ———————                           0.035
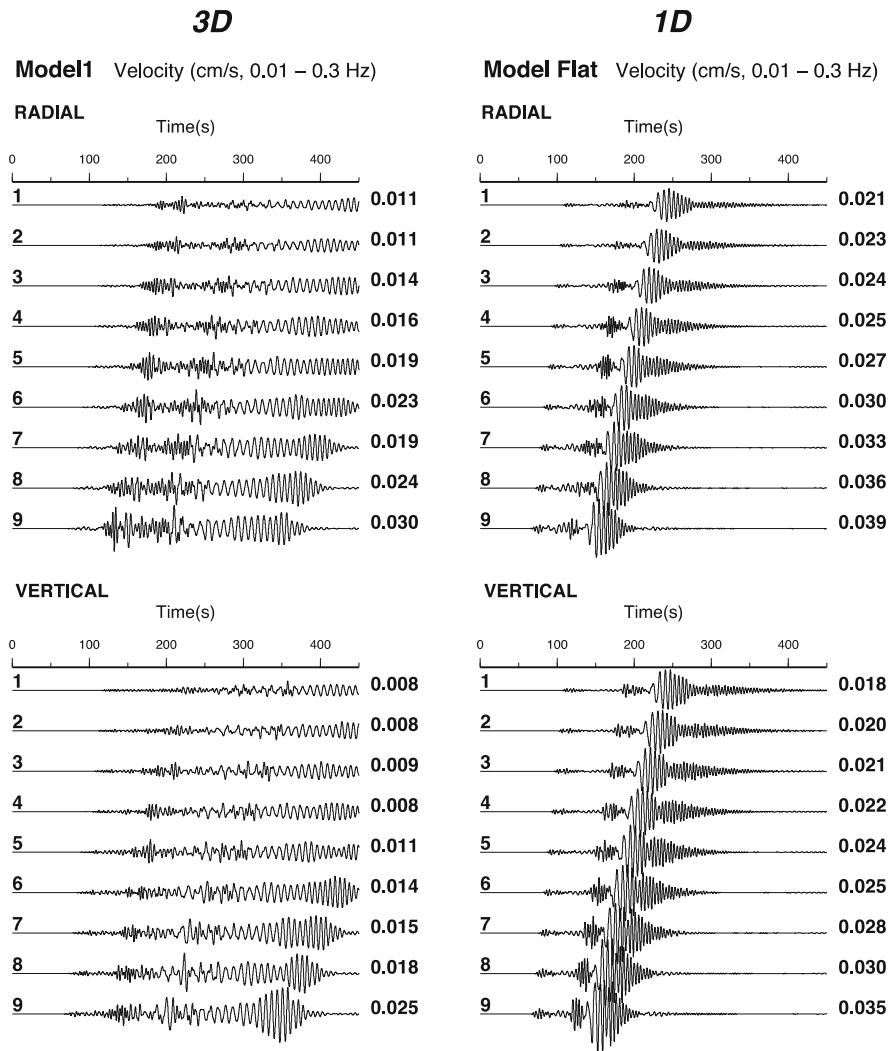
Figure 10

Comparison of synthetic velocity seismograms computed using a 3D model (Model 1, *left panels*) and a 1D model (*right panels*) for a double-couple point source with thrust focal mechanism. The seismograms are band-pass filtered at 0.01–0.3 Hz

the basin edge in Model 3, and its location above the source facilitates trapping of waves that enter the basin. The basin-guided wave effect increases the amplitude of ground motion. This distance-dependent effect can also be seen in the acceleration response spectra computed for the radial component of motion, shown in Figs. 9, 10. The response spectra show a larger separation at stations 1, 2, and 3, located near the western edge of the basin. The differences among models are larger at short periods, smaller than 3 s.

Our simulation results suggest that the basin structure on the east side of the Gulf affects the

ground motion on the west side of the Gulf, especially at short periods. We also found that, at these periods, the effect of shallow basin structure is significant in the vertical component of motion (Fig. 8b).

The effect of 3D structure on ground motion at basin sites becomes very clear when we compare synthetic seismograms computed with a 3D basin model (Model 1) and a 1D reference velocity model. The 1D-layered model was derived from the velocity structure below station 1 in Model 1. The comparison of synthetic seismograms obtained with the 3D and

1D models is shown in Fig. 10. The comparison suggests that the effect of 3D basin structure causes the increase of ground motion duration. The ground motion generated with 3D basin models is dominated by secondary surface waves with durations that depend on station location. In contrast, the 1D model creates dispersive surface waves that are confined within a relatively short time window, after the body waves. This numerical experiment demonstrates that ground motion produced with 1D regional velocity models of the Gulf basin may produce unrealistic ground motion. The seismograms will lack the energetic basin-induced surface waves with very long duration enhanced by 3D wave scattering.

## 6. Conclusions

This study is an attempt to analyze ground motion characteristics observed in the western side of the Arabian Gulf from earthquakes in the Zagros Mountains using comparisons with GMPEs and ground motion simulation. The comparisons with GMPEs showed that ground motion recorded in the Gulf region from earthquakes in the Zagros Mountains region is anomalous. The ground motion response in the period range of 5–10 s is much higher than the predicted one, with factors approaching 100, depending on the station and event locations. In contrast, at shorter periods the ground motion response is lower by at least a factor of 2. The extraordinary long duration of the seismic energy observed in the intermediate and long-period bands may have a significant impact on large structures along the Gulf shoreline. We speculate that the duration and amplitude of ground motion is due to waveguide effects in the sedimentary structure of the Gulf basin.

This hypothesis was tested using large-scale 3D waveform modeling. Sensitivity analysis of the basin induced waves and the corresponding response spectra due to shallow complexities in the basin models reveal the significant implication of basin structure in predicting strong ground motion in the Gulf region. Our high performance computer simulations suggest that a plausible explanation of the anomalous observed ground motion is the generation

of basin reverberation waves that are trapped in the shallow sedimentary layers of the basin. Non-uniform structural effects on wave propagation cause the basin response to be period-dependent and highly variable. In order to reproduce the extremely long duration of the observed ground motion our simulations required a $Q_p = 200$ and $Q_s = 100$ in the top sedimentary layers of the basin. These relatively high-quality factors imply that long-period (2–10 s) waves are subject to rather low attenuation when propagating in the Gulf basin. The observation of strongly path-dependent amplitudes in the basin structure suggest that this region might be a good natural laboratory to test numerical simulation of ground motions to predict motions in the 1–10 s period band. Rapid development of infrastructure, including tall buildings, bridges, pipelines, and ports in this region will likely expose the region to seismic risk and further indicate that improved seismic hazard analysis of long-period motions is warranted.

The simulation results confirm our hypothesis that long-period waves with extremely long duration and relatively large amplitudes are caused by the geometry of the basin sedimentary layers and, to some extent, by the relatively shallow earthquake depth in the Zagros mountains, which favors the channeling of more seismic energy into the shallow sedimentary layers. Combined effects of basin edge geometry with sharp velocity contrast, and shallow earthquakes (depth <10 km) on the eastern part of the Arabian Gulf can cause large long-period ground motion on the western part of the Gulf. This study is a first step toward understanding and characterizing ground motion in the eastern part of the Gulf from earthquakes in the Zagros Mountains region. The development of well-constrained and high-resolution crustal velocity models of the region is crucial for improving the quality of earthquake ground motion prediction on a broad period range.

Both GMPEs adopted in this study may not be reliable at very long distances. Nevertheless, we used them as a reference to show the extremely large difference between recorded and predicted ground motion observed at all stations. More strong motion stations are need in order to develop adequate GMPEs, and improve strong ground motion characterization for the region.

## Acknowledgments

The authors would like express their gratitude to the National Plan for Science, Technology, and Innovation at King Abdulaziz City for Science and Technology (KACST), Saudi Arabia, for funding this project (Grant No. 09–INF945-02). The authors would like to thank two anonymous reviewers for their comments and suggestions which greatly improved the clarity of the manuscript. Numerical simulations were performed on the SIERRA and CAB Linux clusters operated by Livermore Computing Center. This work was performed under the auspices of the U.S. Department of Energy by Lawrence Livermore National Laboratory under Contract DE-AC52-07NA27344. Some figures in this paper were drawn using Generic Mapping Tools software package developed by WESSEL and SMITH (1998).

**Open Access** This article is distributed under the terms of the Creative Commons Attribution License which permits any use, distribution, and reproduction in any medium, provided the original author(s) and the source are credited.

## REFERENCES

AAGAARD, B., et al. (2008), Ground motion modeling of the 1906 San Francisco earthquake II: Ground motion estimates for the 1906 earthquake and scenario events, Bull. Seismol. Soc. Am., 98, 10121046, doi:10.1785/0120060410.

AL-AMRI, A. M. (2013). Seismotectonics and seismogenic source zones of the Arabian Platform, K. Al Hosani et al. (eds.), Lithosphere Dynamics and Sedimentary Basins: The Arabian Plate and Analogues, Frontiers in Earth Sciences, doi:10.1007/978-3-642-30609-9-15, Springer-Verlag Berlin Heidelberg.

AL-AMRI, A.M. (1999). The crustal and upper-mantle structure of the interior Arabian platform, Geophysical Journal International, 136, 421–430.

AL-AMRI, A.M. (1998). The crustal structure of the western Arabian Platform from the spectral analysis of long-period P-wave amplitude ratios, Tectonophysics, 290, 271–283.

AL-AMRI, A. L, R. MELLORS, and F. L. VERNON (1999). Broadband Seismic Noise Characteristics of the Arabian Shield, Arabian Journal of Science and Engineering, King Fahd University of Petroleum and Minerals, 24, 99–113.

AL-AMRI, A.M. A. J. RODGERS, and T. A. AL-KHALIFAH (2008). Improving the level of seismic hazard parameters in Saudi Arabia using earthquake location. Arab J Geosci. 1, 1, 1–15.

AL-DAMEGH, K., SANDVOL, E., AL-LAZKI, A. and BARAZANGI, M. (2004). Regional wave propagation (Sn and Lg) and Pn attenuation in the Arabian plate and surrounding regions, Geophys. J. Int., 157, 775–795.

ALSINAWI, S. A., 1986. Historical Seismicity of the Arab Region. Proceedings of the Third Arab Seismological Seminar, Riyadh Saudi Arabia, pp. 11–33.

AMBRASEYS N. N., 1988. The seismicity of Saudi Arabia and adjacent area, Report Prepared for the Kingdom of Saudi Arabia. ESEE, Imperial Col. Sci. Tech., London, U.K. Report 88/11. p. 294.

AMBRASEYS, N. N.; MELVILLE, C.P. and ADAMS, R. D., 1994. The Seismicity of Egypt, Arabia and the Red Sea-A historical review. Cambridge University Press and King Abdul Aziz City for Science and Technology, p. 181.

APPELO, D., and N. A. PETERSSON (2008), A stable finite difference method for the elastic wave equation on complex geometries with free surfaces, Commun. Comput. Phys., 5, 84–107.

BASSIN, C. G. LASKE, and G. MASTERS (2000). The current limits of resolution in surface wave tomography in North America, EOS Trans. AGU, F897, 81.

BOORE and ATKINSON (2006), Earthquake Ground-Motion Prediction Equations for Eastern North America. Bull. Seism. Soc. Am., 96, no 6, 2181–2205.

CAMPBELL and BOZORGNIA (2008) NGA ground motion model for the geometric mean horizontal component of PGA, PGV,PGD and 5% damped linear elastic response spectra for periods ranging from 0.01 to 10 s. Earthquake Spectra, 24, No. 1, 139–171.

FRANKEL, A., R. W. CLAYTON (1986). Finite Difference Simulations of Seismic Scattering: Implications for the Propagation of Short-Period Seismic Waves in the Crust and Models of Crustal Heterogeneity. JGR, Vol. 91, B6, 6465–6489.

GÖK, R., H. MAHDI, H. AL-SHUKRI and A. RODGERS (2008). Crustal structure of Iraq from receiver functions and surface wave dispersion, Geophys. Journal Int., Vol. 172(3), pp. 1179–1187.

JOHNSON, P.R. (1998). Tectonic Map of Saudi Arabia and Adjacent Areas, Ministry of Petroleum and Mineral Resources, Deputy Ministry Mineral, Resources Technical Report USGS-TR-98-3, Jeddah, Saudi Arabia.

LASKE, G. and T.G. MASTERS (1997). A global digital map of sediment thickness, EOS Trans. AGU, 78, F483, http://igppweb.ucsd.edu/~gabi/sediment.html.

MELLORS, R., VERNON, F., CAMP, V., AL-AMRI, A.M K GHARIB, A. (1999). Regional waveform propagation in the Saudi Arabian Peninsula and evidence for a hot upper mantle under western Arabia. J. Geophys. Res., 104, 20,221–20,235.

MOONEY, W.D., G. LASKE, and G. MASTERS (1998). CRUST5.1: A global crustal model at 5° × 5°, J. Geophys. Res., 103, 727–747.

NILSSON, S., N. A. PETERSSON, B. SJOGREEN, and H.-O. KREISS (2007), Stable difference approximations for the elastic wave equation in second order formulation, SIAM J. Numer. Anal., 45, 1902–1936, doi:10.1137/060663520.

PASYANOS, M.E., W. R. WALTER, E. M. MATZEL (2009). A simultaneous multiphase approach to determine P-wave and S-wave attenuation of the Crust and upper Mantle. Bull. Seism. Soc. Am., 99, 3314–3325.

PASYANOS, M.E., T.G. MASTERS, G. LASKE, and Z. MA (2014). LITHO1.0: An updated crust and lithospheric model of the Earth, J. Geophys. Res. Solid Earth, 119, 2153–2173, doi:10.1002/2013JB010626.

PETERSSON, N. A., and B. SJOGREEN (2010a), Reference guide to WPP version 2.0, Tech Rep. LLNL-TR-422928, Lawrence Livermore Natl. Lab., Livermore, Calif.

PETERSSON N.A., and B. SJOGREEN (2010b). Stable grid refinement and singular source discretization for seismic wave simulations.

Communications in Computational Physics, vol. 8, no. 5, pp. 1074–1110.

PITARKA, A., K. IRIKURA, T. IWATA and H. SEKIGUCHI (1998). *Three-dimensional simulation of the near-fault ground motion for the 1995 Hyogo-ken Nanbu (Kobe), Japan, earthquake*. Bull. Seism. Soc. Am., *88*, 428–440.

RODGERS, A.J, A. FOWLER, A.S. AL-AMRI, and A. AL-ENEZI (2006). *The March 11, 2002 Masafi, United Arab Emirates earthquake: Insights into the seismotectonics of the northern Oman Mountains*. Tectonophysics, *415* (2006) 57–64.

RODGERS, A., W. WALTER, R. MELLORS, A. M. S. AL-AMRI and Y. S. ZHANG (1999). *Lithospheric structure of the Arabian Shield and Platform from complete regional waveform modeling and surface wave group velocities*, Geophys. J. Int., *138*, 871–878.

RODGERS, A., J.F. NI, and T. M. HEARN (1997). *Propagation characteristics of short-period Sn and Lg in the Middle East*, Bull. Seism. Soc. Am. *87*, 396–413.

TALEBIAN, M., and J. JACKSON (2004), *A reappraisal of earthquake focal mechanisms and active shortening in the Zagros mountains of Iran*, Geophys. J. Int., *156*, 506–526.

TKALČIČ H., M. PASYANOS, A. RODGERS, R. GOK and A. AL-AMRI (2006). *A multi-step approach for joint modeling of surface wave dispersion and teleseismic receiver functions: Implications for lithospheric structure of the Arabian Peninsula*. J. Geophys. Res., *111*, B113111, doi:10.1029/2005JB004130.

WESSEL; P, W.H.F. SMITH (1998). *New improved version of generic mapping tools released*. EOS Trans. Amer. Geophys. Union *79* (47):579. doi:10.1029/98EO00426.